R and D CENTER LABORATORY

TECHNICAL REPORT

NO. 12643

OPTIMIZATION OF FORCE BALANCING MECHANISMS

Contract Number DAAK 30-80-C-0042

MARCH 1982

Doo Y. Jo and Edward J. Haug
College of Engineering
The University of Iowa
Iowa City, IA 52242
University of Iowa Report No. 81-6

by Ronald R. Beck, Project Engineer, TACOM
US Army Tank-Automotive Command
ATTN: DRSTA-ZSA
Warren, MI 48090

U.S. ARMY TANK-AUTOMOTIVE COMMAND
RESEARCH AND DEVELOPMENT CENTER
Warren, Michigan 48090

NOTICES

The findings in this report are not to be construed as an official Department of the Army position.

Mention of any trade names or manufacturers in this report shall not be construed as advertising nor as an official endorsement of approval of such products or companies by the U.S. Government.

Destroy this report when it is no longer needed. Do not return it to originator.

REPORT DOCUMENTATION PAGE

READ INSTRUCTIONS BEFORE COMPLETING FORM

1. REPORT NUMBER: 12643	2. GOVT ACCESSION NO.
3. RECIPIENT'S CATALOG NUMBER	
4. TITLE (and Subtitle): Optimization of Force Balancing Mechanism	5. TYPE OF REPORT & PERIOD COVERED
	6. PERFORMING ORG. REPORT NUMBER
7. AUTHOR(s): Doo Y. Jo, Edward J. Haug, University of Iowa; Ronald R. Beck, TACOM	8. CONTRACT OR GRANT NUMBER(s): DAAK 30-80-C-0042
9. PERFORMING ORGANIZATION NAME AND ADDRESS: The University of Iowa, College of Engineering, Iowa City, IA 52242	10. PROGRAM ELEMENT, PROJECT, TASK AREA & WORK UNIT NUMBERS
11. CONTROLLING OFFICE NAME AND ADDRESS: US Army Tank-Automotive Command, R&D Center, Tank-Automotive Concepts Lab, DRSTA-ZSA, Warren, MI 48090	12. REPORT DATE: March 1982
	13. NUMBER OF PAGES: 37
14. MONITORING AGENCY NAME & ADDRESS(if different from Controlling Office)	15. SECURITY CLASS. (of this report): UNCLASSIFIED
	15a. DECLASSIFICATION/DOWNGRADING SCHEDULE

16. DISTRIBUTION STATEMENT (of this Report)

Approved for public release; distribution unlimited.

17. DISTRIBUTION STATEMENT (of the abstract entered in Block 20, if different from Report)

18. SUPPLEMENTARY NOTES

19. KEY WORDS (Continue on reverse side if necessary and identify by block number)

20. ABSTRACT (Continue on reverse side if necessary and identify by block number)

A theory and computer code for design optimization of force-balancing mechanisms is developed. The force-balancing mechanisms treated in this report use linear elastic force elements. A constrained, multi-element formulation is introduced to analyze kinematics of mechanisms. Two joint formulations, revolute and translational, are introduced. The optimal design problem is formulated as a descretized problem. The objective of the optimization problem is to minimize the largest force required to move the

mechanism through its path. A gradient projection method is adopted for optimization. Example calculations are presented for a mechanical spring Weapon Equalibrator. A substantial reduction (60%) of the cost function is demonstrated, compared with conventional equalibrator design methods.

TABLE OF CONTENTS

CHAPTER		Page
1.	INTRODUCTION	1
1.1	Force-Balancing Mechanisms	1
1.2	Static Force-Balancing Mechanism	3
1.3	Linear Equilibrator	3
2.	STATIC ANALYSIS OF MECHANISMS	5
2.1	Constrained Multi-Element Formulation	5
2.2	State Equation	5
2.3	Kinematic Constraint Equations for Typical Joints	9
2.3.1	Revolute Joint	9
2.3.2	Translational Joint	11
3.	DERIVATION OF GENERALIZED FORCE FOR A LINEAR SYSTEM	14
4.	OPTIMAL DESIGN PROBLEM FORMULATION	22
4.1	Statement of the Optimal Design Problem	22
4.2	Discretized Problem	22
4.3	A Reformulation of the Problem	23
4.4	Design Sensitivity Analysis	24
4.5	Optimization Algorithm	27
5.	APPLICATIONS	30
5.1	A Linear Mechanical Spring Weapon Equilibrator	30
REFERENCES		37

CHAPTER 1

INTRODUCTION

Among various kinds of mechanisms, there is a certain group called force-balancing mechanisms. This report aims to develop a general purpose theory and a computer code for design optimization of force-balancing mechanisms and to provide example calculations.

1-1 Force-Balancing Mechanisms

A force-balancing mechanism has a device or counterweight that maintains the mechanism in a force-balance state, or at least minimizes the force necessary to drive the mechanism over a certain range of inputs. Figure 1-1 shows an example of a force-balancing mechanism that couples an automobile hood to the body. It is a 6 bar linkage with a linear mechanical spring. One can open or close the hood easily because the spring of the mechanism exerts a balancing force against the weight of the hood.

Figure 1-2 shows a schematic diagram of an elevating mechanism of a weapon with an equilibrator. Preponderance of the tipping parts is inevitable in some applications, hence an equilibrator is essential for minimizing elevating or depressing effort. The weight moment increases as the tipping parts are lowered, so the equilibrator is designed to exert a larger balancing force when the elevation angle is small than when it is large.

Figure 1-3 shows a sliding door with a torsional spring equilibrator. The counterweight of an elevator system is another example of a force-balancing mechanism.

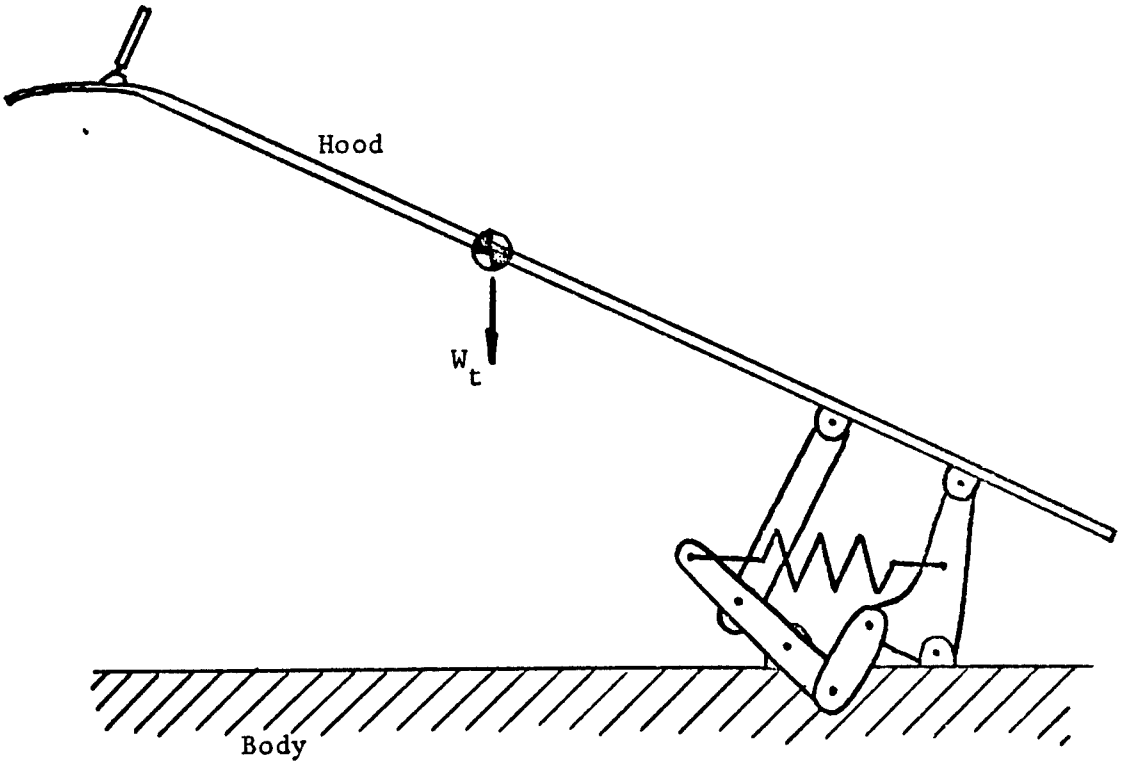

Figure 1-1 Force-Balancing Mechanism of an Automobile Hood

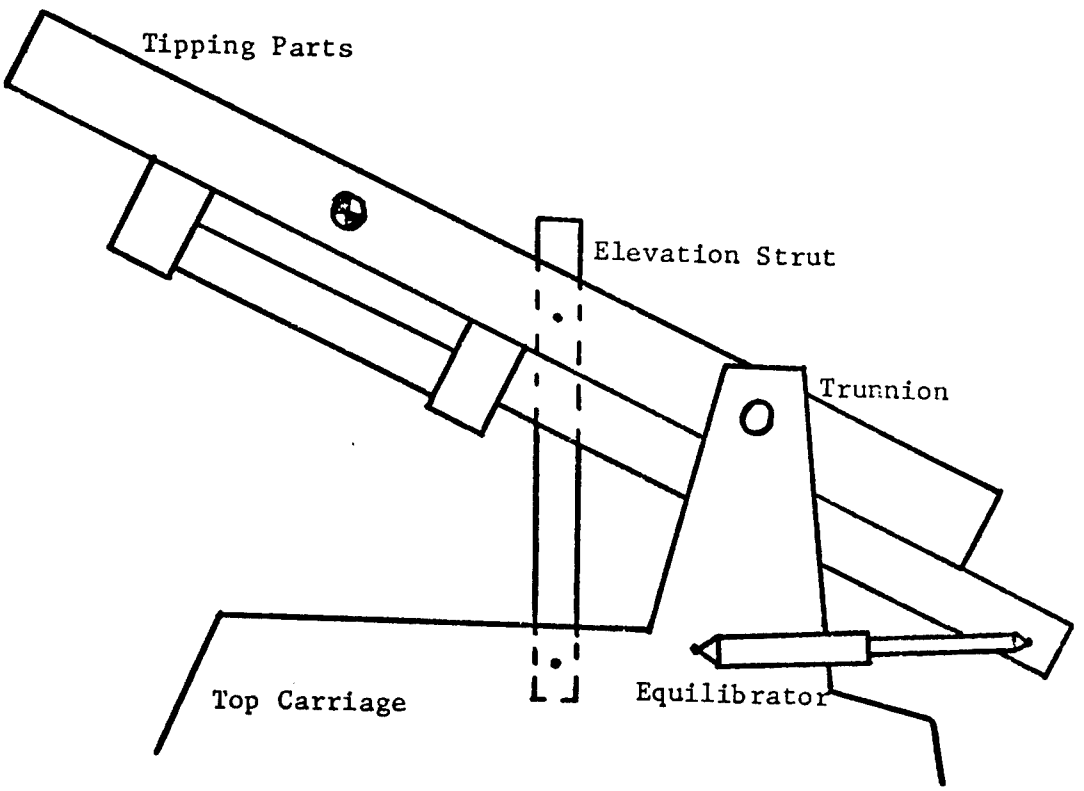

Figure 1-2 Equilibrator for an Unbalanced Weapon

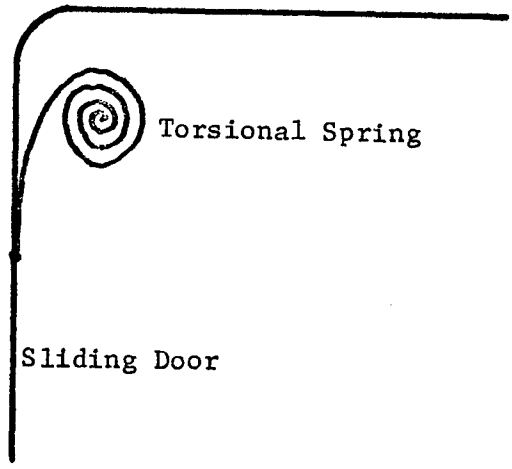

Figure 1-3 Sliding Door with a Torsional Spring Equilibrator

1-2 Static Force-Balancing Mechanism

As described briefly in the previous paragraph, the force-balancing mechanisms are intended to maintain parts in a desired position. Although the balancing force is exerted during motion of the mechanism, the motion is slow. Therefore, the force-balancing mechanism can be termed a static force-balancing mechanism. Once the range of motion is discretized (see par. 4.2), then the mechanism is analyzed at each input point as a static case. Hence, the term static force-balancing mechanism is quite natural.

1-3 Linear Equilibrator

To avoid being too broad, this report deals only with static force-balancing mechanisms that have linear spring equilibrators. As the word "linear" implies, the equilibrator has linear characteristics. The equilibrator may be a linear mechanical spring, pneumatic spring, or

torsional spring. The magnitude of the force exerted by the equilibrator is proportional to the change of displacement; i.e., the balancing force is

$$F = K \Delta \ell \tag{1-1}$$

where F = balancing force or torque

K = constant spring rate

$\Delta \ell$ = linear or angular displacement

In most cases, the force necessary to equilibrate a mechanism is non-linear, while the equilibrating force available is linear. Therefore, perfect balancing is impossible over the entire range of motion. This fact leads to a problem of worst case optimization (see Ref. 1, Ch. 3, or Ref. 2), which is closely related to min-max theory (see Ref. 1).

To solve the equations for determining the state of a mechanism, a technique based on the DADS formulation (see Ref. 2) is used. Using the DADS formulation, one can minimize the computational difficulty of solving highly nonlinear equations.

CHAPTER 2

STATIC ANALYSIS OF MECHANISMS

For obtaining the equations determining the state of a mechanism, a constrained multi-element formulation is described in this section. Kinematic constraint equations for the most common joints used in mechanisms are derived as state equations.

2-1 Constrained Multi-Element Formulation

Figure 2-1 shows the ith body of a mechanical system that lies in an inertial x-y reference frame. A local coordinate system (ξ_i, η_i) is embedded in the body. The position of the local coordinate system is arbitrary, but is usually located at the center of mass. The position and orientation of the body are described by three generalized coordinates; x_i, y_i, and θ_i.

The constrained multi-element formulation regards joints connecting two bodies as constraints imposed on the relative motion of the connected bodies. By doing this, the method is capable of modeling open or closed loop systems. However, because each joint (revolute joint and translational joints are most common) brings forth two additional constraint equations, it gives rise to a larger number of equations than other methods.

2-2 State Equation

Consider a system with n bodies connected by ℓ joints in the plane. Each body has three generalized coordinates, x, y, and θ. Hence a system of n bodies has a total of 3n generalized coordinates. As stated in the previous paragraph, a joint is regarded as a constraint on the motion of the pair of bodies that the joint connects. The most common joints (revolute

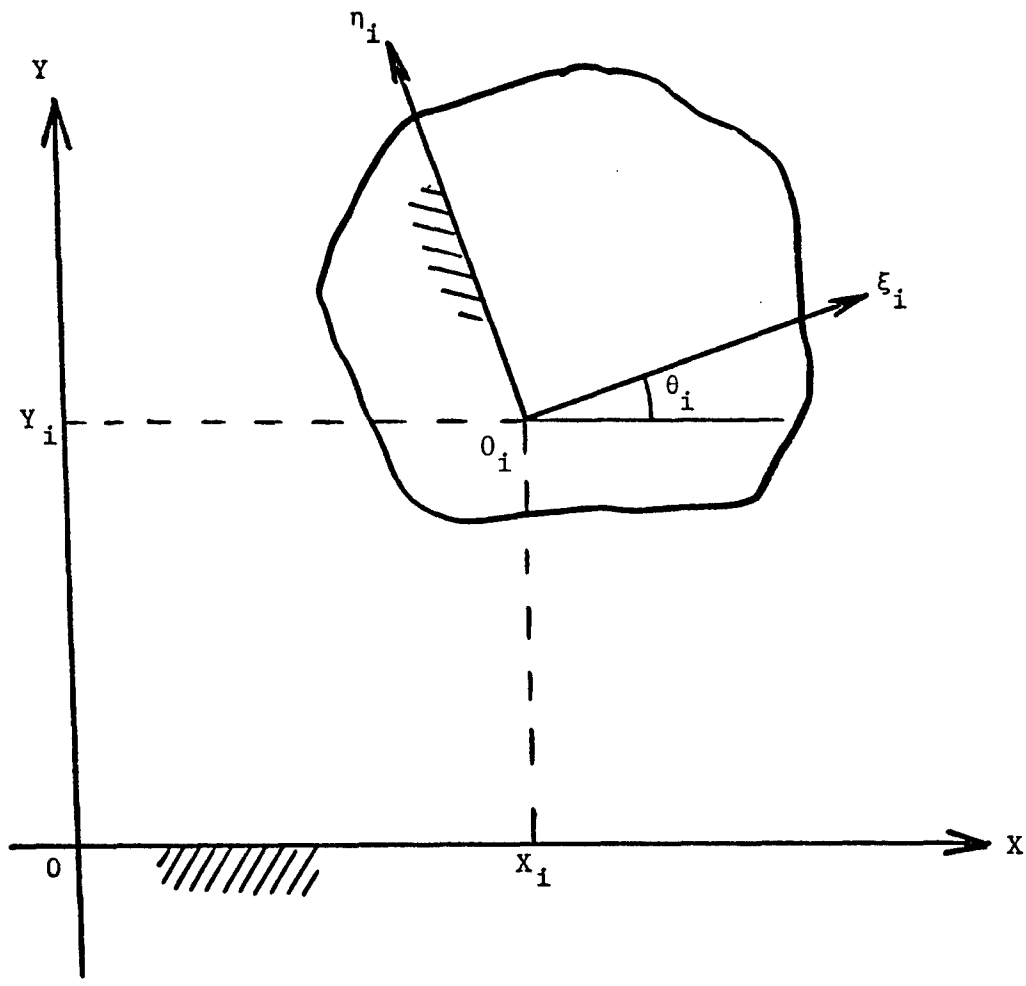

Figure 2-1 Definition of the Generalized Coordinate of the ith Body

and translational) are dealt with, each joint having two constraint equations. The constraint equations express necessary conditions that the two bodies must satisfy to be compatible with the joints. A system that has ℓ independent joints has 2ℓ constraint equations. Thus, the number of free degrees-of-freedom of this system is $m = 3n - 2\ell$. The condition $m > 0$ must be satisfied by all kinematic systems. The 3n degrees-of-freedom are denoted by $z \in R^{3n}$, $z = [x_1, y_1, \theta_1, x_2, \ldots, x_n, y_n, \theta_n]^T$. Since the components of the vector z describe the state of the system, they are called state variables and z is called state vector. The 2ℓ constraint equations are the kinematic conditions that the state must satisfy, thus these constraint equations are called kinematic constraint equations and can be written as

$$\Phi^k(z, b) = 0 \tag{2-1}$$

where

$$\Phi^k(z, b) = \begin{bmatrix} \phi_1^k(z, b) \\ \vdots \\ \phi_{2\ell}^k(z, b) \end{bmatrix}$$

and $b \in R^k$ is a vector of design variables.

The basic purpose of designing a kinematic system is to obtain a system that allows the transmission of motion or force from an input link to an output link. The mechanism can only be given input motion through a set of free degrees-of-freedom, which is specified as a function of some free parameter, or as some relationship between the 3n state variables. Since all degrees-of-freedom must be specified to drive the mechanism, m additional driving equations of constraint are required, in the form

$$\Phi^d(z, b, \alpha) = 0 \tag{2-2}$$

where

$$\Phi^d(z,\ b,\ \alpha) = \begin{bmatrix} \phi_1^d(z,\ b,\ \alpha) \\ \vdots \\ \phi_m^d(z,\ b,\ \alpha) \end{bmatrix}$$

and $\alpha \in R^p$ is a vector of environmental parameters (see Ref. 1, Ch. 3). The range of motion is specified by α. For example, consider a four-bar-linkage of Fig. 2-2. This mechanism has one free degree-of-freedom. Hence, α could be the angle of the input link with respect to the ground. Thus α specifies the position at which the mechanism is being analyzed.

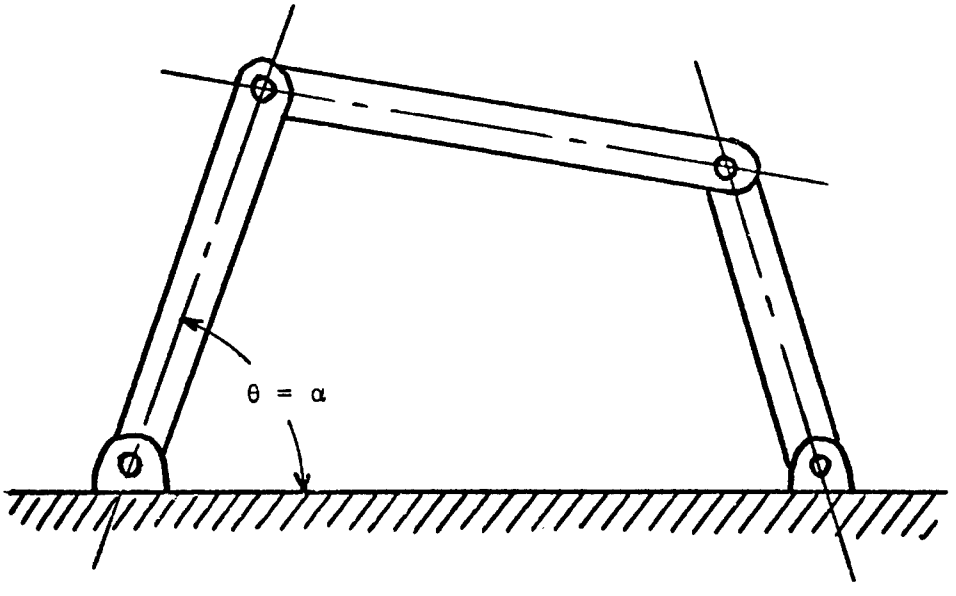

Figure 2-2 Four-Bar-Linkage with One Degree-of-Freedom

Combining Eqs. 2-1 and 2-2, one has 3n constraint equations, which can be written in the form

$$\Phi(z,\ b,\ \alpha) = \begin{bmatrix} \Phi^k(z,\ b) \\ \Phi^d(z,\ b,\ \alpha) \end{bmatrix} = 0 \qquad (2\text{-}3)$$

Equation 2-3 is the state equation for position analysis of the mechanism. Of all the variables in Eq. 2-3, design variables b and environmental parameters α, are specified before any attempt is made to solve the equations for the state z. Thus, Eqs. 2-3 are interpreted as 3n equations with 3n unknowns z. This system can be solved uniquely for $z(b, \alpha)$, provided that the implicit function theorem (Ref. 3) is satisfied; i.e., the matrix

$$\frac{\partial \Phi}{\partial z} = \left[\frac{\partial \phi_i}{\partial z_j}\right]_{3n \times 3n}$$

is nonsingular.

2-3 Kinematic Constraint Equations for Typical Joints

2-3.1 Revolute Joint

Figure 2-3 shows two adjacent bodies (i and j) that are connected by revolute joints. The local coordinate systems (ξ_i, η_i) and (ξ_j, η_j) are embedded in each body and located by x_i, y_i, θ_i and x_j, y_j, θ_j, with respect to the global (x, y) coordinate system. The origins of the local coordinates are positioned by $\vec{R}_i$ and $\vec{R}_j$, with respect to global coordinates.

Consider two points P_{ij} on the ith body and P_{ji} on the jth body that are located by $\vec{r}_{ij}$ and $\vec{r}_{ji}$ with respect to the local coordinate system. The connection of P_{ij} and P_{ji} is expressed by a vector $\vec{r}_p$. Executing a closed loop from the origin of the global coordinate yields the vector relationship

$$\vec{R}_i + \vec{r}_{ij} + \vec{r}_p - \vec{r}_{ji} - \vec{R}_j = 0 \qquad (2\text{-}4)$$

The kinematic constraint equations for a revolute joint can be obtained by requiring that $\vec{r}_p = 0$; i.e., requiring that P_{ij} coincide with P_{ji}. Using

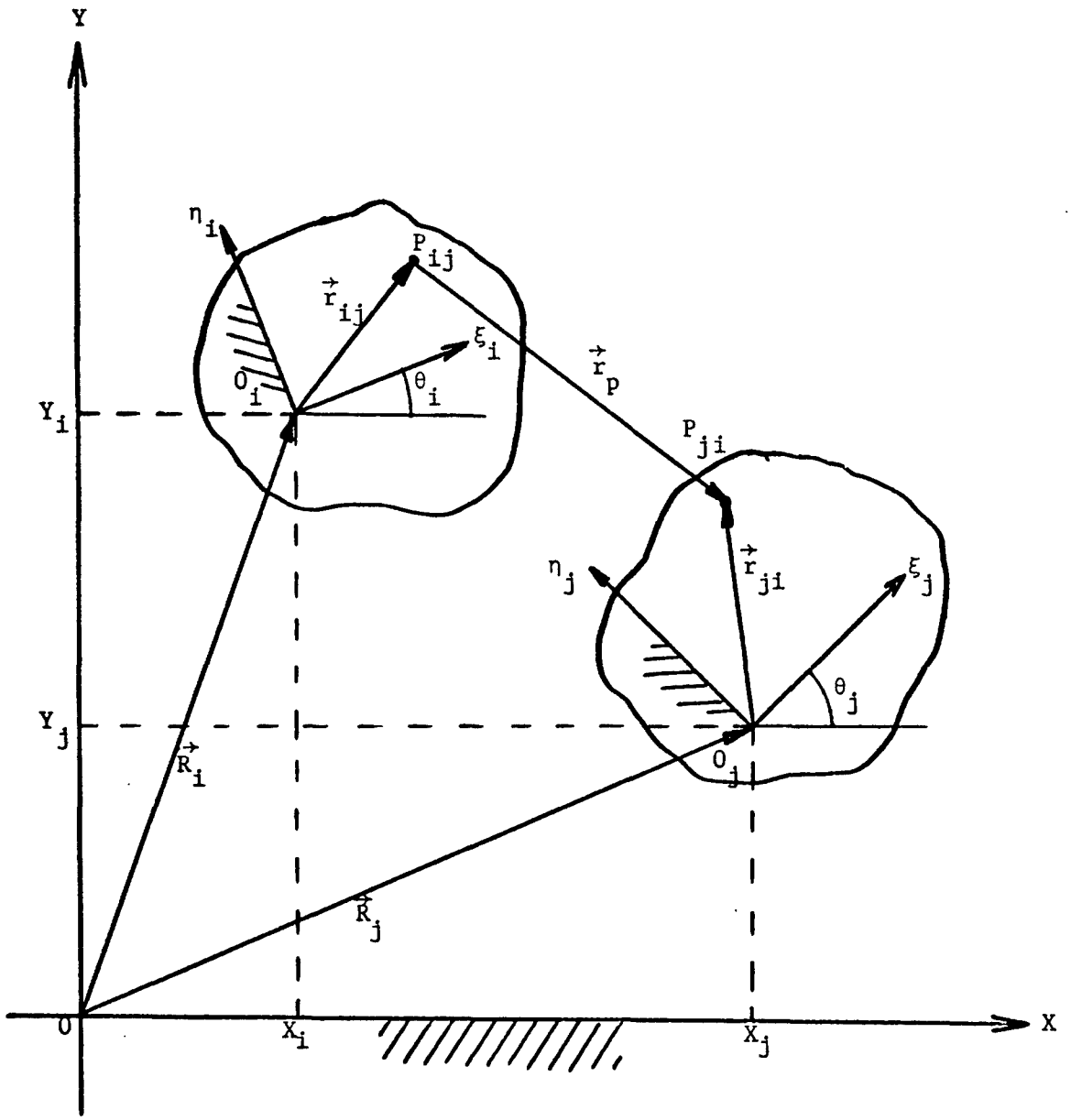

Figure 2-3 Revolute Joint Coordinates

the proper coordinate transformation, Eq. 2-4 can be written as

$$\left.\begin{aligned} \phi_x &= X_i + \xi_i\cos\theta_i - \eta_i\sin\theta_i - X_j - \xi_j\cos\theta_j \\ &\quad + \eta_j\sin\theta_j = 0 \\ \phi_y &= Y_i + \xi_i\sin\theta_i + \eta_i\cos\theta_i - Y_j - \xi_j\sin\theta_j \\ &\quad - \eta_j\cos\theta_j = 0 \end{aligned}\right\} \qquad (2\text{-}5)$$

2-3.2 Translational Joint

Figure 2-4 shows the geometry of a translational joint. Definitions of the local coordinates and position vectors are similar to those of a revolute joint in the previous paragraph. The translational joint is defined by requiring that the vector $\vec{r}_p$ be parallel to the path of relative motion between the two bodies, where $\vec{r}_p$ is the vector between two points P_{ij} and P_{ji} that are located by two nonzero vectors $\vec{r}_{ij}$ and $\vec{r}_{ji}$ that are perpendicular to the line of relative motion. From Eq. 2-4,

$$\vec{r}_p = -(\vec{R}_i + \vec{r}_{ij}) + (\vec{R}_j + \vec{r}_{ji})$$

The condition that the vector $\vec{r}_{ij}$ is perpendicular to the vector $\vec{r}_p$ gives one constraint equation as

$$\vec{r}_p \cdot \vec{r}_{ij} = 0 \qquad (2\text{-}6)$$

The second constraint equation is obtained by noting that $\vec{r}_{ij}$ and $\vec{r}_{ji}$ are parallel to each other; i.e.,

$$\vec{r}_{ij} \times \vec{r}_{ji} = \vec{0} \qquad (2\text{-}7)$$

Equations 2-6 and 2-7 can be rewritten in scalar form as

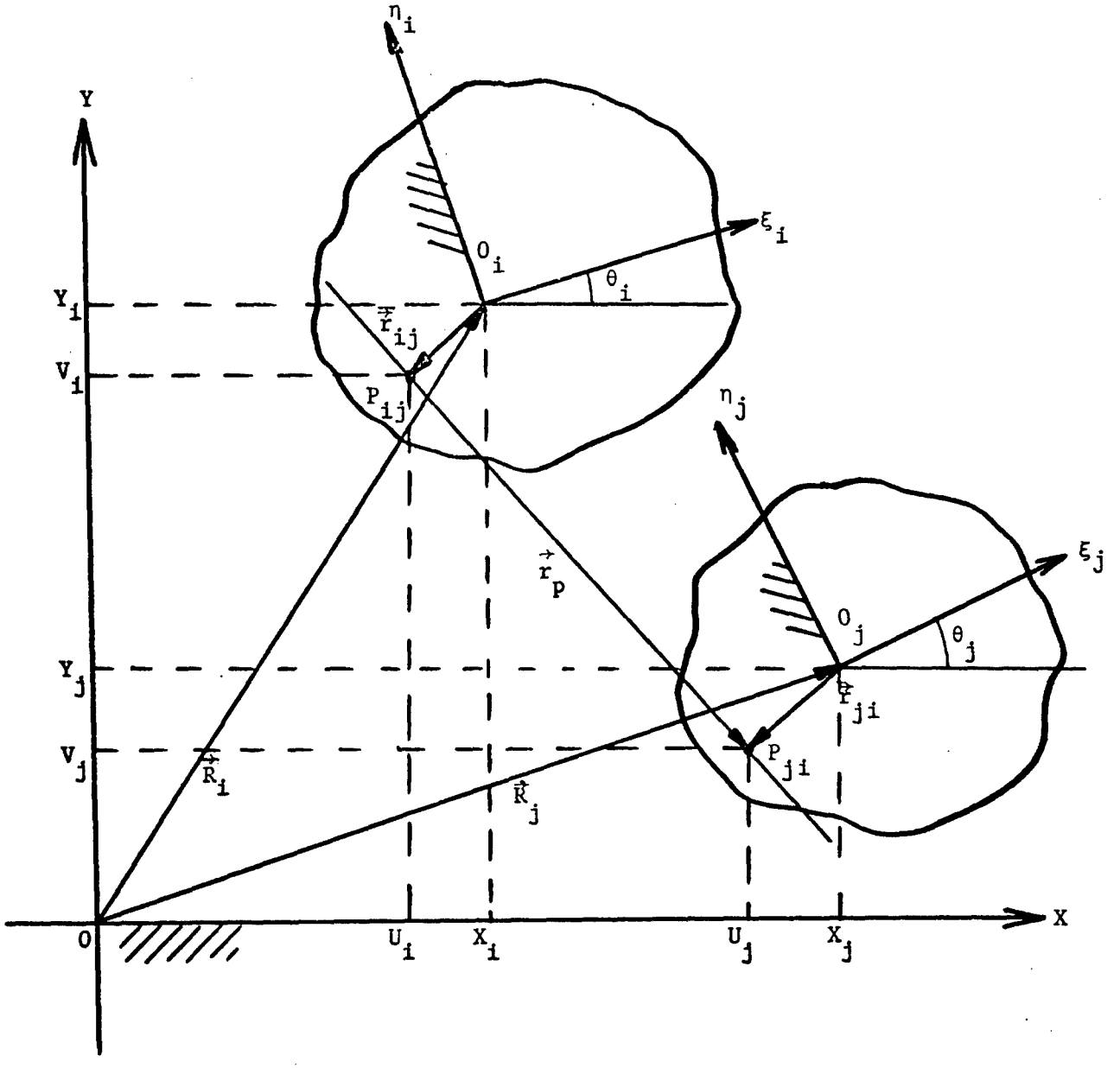

Figure 2-4 Translational Joint Coordinates

$$\left.\begin{aligned} \phi_n &= (U_i - X_i)(U_i - U_j) + (V_i - Y_i)(V_i - V_j) = 0 \\ \phi_\theta &= (U_i - X_i)(V_j - Y_j) - (V_i - V_i)(U_j - X_j) = 0 \end{aligned}\right\} \qquad (2\text{-}8)$$

where

$$U_i = X_i + \xi_i \cos\theta_i - \eta_i \sin\theta_i$$

$$U_j = X_j + \xi_j \cos\theta_j - \eta_j \sin\theta_j$$

$$V_i = Y_i + \xi_i \sin\theta_i + \eta_i \cos\theta_i$$

$$V_j = Y_j + \xi_j \sin\theta_j + \eta_j \cos\theta_j$$

Equations 2-8 are the constraint equations for the translational joint.

CHAPTER 3

DERIVATION OF GENERALIZED FORCE FOR A LINEAR SYSTEM

Consider a system of n bodies that has m linear equilibrators and s torsional spring equilibrators. A system that has linear force-balancing elements is called a linear system in this Chapter. Figure 3-1 shows adjacent ith and jth bodies, with the kth linear equilibrator element and the qth torsional equilibrator element. The definition and location of local coordinates of each body are similar to those for a revolute joint. However, in this system the kth linear spring equilibrator is connecting the ith and jth bodies. The attachment points P_{ik} and P_{jk} are located by vectors $\vec{r}_{ik}$ and $\vec{r}_{jk}$, with respect to each body fixed coordinate system. The qth torsional spring equilibrator is installed in ith body. The length of the linear spring equilibrator is expressed as ℓ_{ijk}. The linear spring equilibrator forces are expressed as $\vec{F}_{ik}$ and $\vec{F}_{jk}$. The torque exerted by a torsional spring equilibrator is expressed as M_{iq}.

Similar to Eq. 2-4, executing a closed loop from the origin of the global coordinate system yields the vector relationship

$$\vec{R}_i + \vec{r}_{ik} + \vec{\ell}_{ijk} - \vec{r}_{jk} - \vec{R}_j = 0 \tag{3-1}$$

From Eq. 3-1, $\vec{\ell}_{ijk}$ can be written as

$$\vec{\ell}_{ijk} = -\vec{R}_i - \vec{r}_{ik} + \vec{R}_j + \vec{r}_{jk} \tag{3-2}$$

The derivation of generalized force starts from the principle of virtual work (see Ref. 4); i.e.,

$$\delta W = 0 \tag{3-3}$$

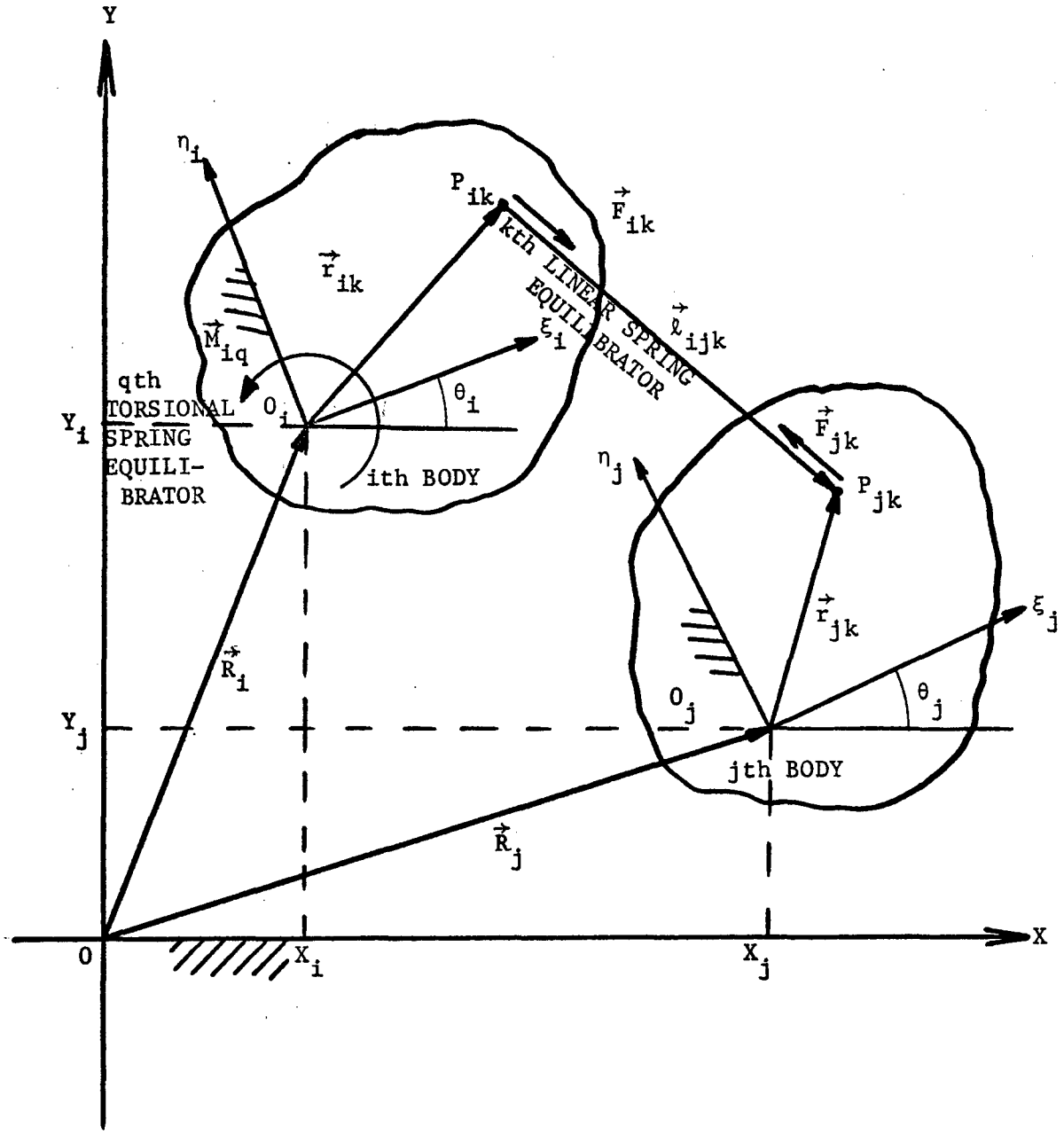

Figure 3-1 Linear Force-Balancing System

The virtual work due to the applied force during the virtual displacement is

$$\delta W = F^T \delta r \tag{3-4}$$

where

F = applied force

δr = virtual displacement

For the force F, the virtual displacement of the point of application of the force is

$$\delta r = \frac{\partial (R_i + r_{ik})}{\partial z} \delta z \tag{3-5}$$

Let the virtual work done by equilibrators and by external forces be δW_{eq} and δW_{ex}, respectively. Then the virtual work done by r linear spring equilibrators and s torsional spring equilibrators is

$$\delta W_{eq} = \sum_{k=1}^{r} \left\{ F_{ik}^T \frac{\partial (R_i + r_{ik})}{\partial z} \delta z + F_{jk}^T \frac{\partial (R_j + r_{jk})}{\partial z} \delta z \right\} + \sum_{q=1}^{s} M_{iq} \frac{\partial \theta_i}{\partial z} \delta z \tag{3-6}$$

The virtual work done by external forces and torques is

$$\delta W_{ex} = \sum_{i=1}^{n} \left\{ \sum_{\ell=1}^{g} P_{i\ell}^T \frac{\partial (R_i + r_{i\ell})}{\partial z} \delta z + \sum_{m=1}^{h} T_{im} \frac{\partial \theta_i}{\partial z} \delta z \right\} \tag{3-7}$$

where

δW_{ex} = virtual work by external forces

$P_{i\ell}$ = ℓth external force on body i

T_{im} = mth external torque on body i

g = number of external forces on body i

h = number of external torques on body i.

The total virtual work is thus

$$\delta W = \delta W_{eq} + \delta W_{ex} \tag{3-8}$$

Farkas Lemma (see Ref. 1) guarantees the existence of a Lagrange multiplier vector $\mu \in R^{3n}$ such that

$$\delta W - \mu^T \delta \Phi = 0 \tag{3-9}$$

where

Φ = the vector of state equations.

Substituting δW_{eq} and δW_{ex} in Eqs. 3-6 and 3-7 in Eq. 3-8 and then δW in Eq. 3-8 into Eq. 3-9 and factorizing δz,

$$\left[\sum_{k=1}^{r} \left\{ F_{ik}^T \frac{\partial (R_i + r_{ik})}{\partial z} + F_{jk}^T \frac{\partial (R_j + r_{jk})}{\partial z} \right\} \right.$$

$$+ \sum_{i=1}^{n} \left\{ \sum_{\ell=1}^{g} P_{i\ell}^T \frac{\partial (R_i + r_{i\ell})}{\partial z} + \sum_{m=1}^{h} T_{im} \frac{\partial \theta_i}{\partial z} \right\}$$

$$\left. + \sum_{q=1}^{s} M_{iq} \frac{\partial \theta_i}{\partial z} - \mu^T \frac{\partial \Phi}{\partial z} \right] \delta z = 0 \tag{3-10}$$

Since Eq. 3-10 holds for arbitrary δz,

$$\sum_{k=1}^{r} \left\{ \frac{\partial (R_i + r_{ik})^T}{\partial z} F_{ik} + \frac{\partial (R_j + r_{jk})^T}{\partial z} F_{jk} \right\}$$

$$+ \sum_{i=1}^{n} \left\{ \sum_{\ell=1}^{g} \frac{\partial (R_i + r_{i\ell})^T}{\partial z} P_{i\ell} + \sum_{m=1}^{h} \frac{\partial \theta_i^T}{\partial z} T_{im} \right\}$$

$$+ \sum_{q=1}^{s} \frac{\partial \theta_i^T}{\partial z} M_{iq} = \frac{\partial \Phi^T}{\partial z} \mu \tag{3-11}$$

Defining the left hand side of Eq. 3-11 as a vector G, Eq. 3-11 can be written as

$$\frac{\partial \Phi^T(z, b, \alpha)}{\partial z} \mu = G(z, \alpha, b) \tag{3-12}$$

where

$$G(z, \alpha, b) = \sum_{k=1}^{r} \left\{ \frac{\partial (R_i + r_{ik})^T}{\partial z} F_{ik} + \frac{\partial (R_j + r_{jk})^T}{\partial z} F_{jk} \right\}$$

$$+ \sum_{q=1}^{s} \frac{\partial \theta_i^T}{\partial z} M_{iq}$$

$$+ \sum_{i=1}^{n} \left\{ \sum_{\ell=1}^{g} \frac{\partial (R_i + r_{i\ell})^T}{\partial z} P_{i\ell} + \sum_{m=1}^{h} \frac{\partial \theta_i^T}{\partial z} T_{im} \right\} \tag{3-13}$$

By Newton's law of motion, $F_{ik} = - F_{jk}$. Hence substituting F_{jk} into Eq. 3-13, and denoting the sum of the first two terms of Eq. 3-13 as $G_{eq}(z, b, \alpha)$,

$$G_{eq}(z, b, \alpha) = \sum_{k=1}^{r} \left\{ \frac{\partial (R_i + r_{ik})^T}{\partial z} F_{ik} - \frac{\partial (R_j + r_{jk})^T}{\partial z} F_{ik} \right\}$$

$$+ \sum_{q=1}^{s} \frac{\partial \theta_i^T}{\partial z} M_{iq} \tag{3-14}$$

Factoring F_{ik}, this is

$$G_{eq}(z, b, \alpha) = \sum_{k=1}^{r} \left\{ \frac{\partial (R_i + r_{ik})^T}{\partial z} - \frac{\partial (R_j + r_{jk})^T}{\partial z} \right\} F_{ik}$$

$$+ \sum_{q=1}^{s} \frac{\partial \theta_i^T}{\partial z} M_{iq} \tag{3-15}$$

which becomes

$$G_{eq}(z, b, \alpha) = \sum_{k=1}^{r} \left\{ \frac{\partial(R_i + r_{ik} - R_j - r_{jk})^T}{\partial z} \right\} F_{ik}$$

$$+ \sum_{q=1}^{s} \frac{\partial \theta_i^T}{\partial z} M_{iq} \qquad (3\text{-}16)$$

Substituting $R_i + r_{ik} - R_j - r_{jk}$ from Eq. 3-2 into Eq. 3-16 yields

$$G_{eq}(z, b, \alpha) = \sum_{k=1}^{r} \frac{\partial(-\ell ijk)^T}{\partial z} F_{ik} + \sum_{q=1}^{m} \frac{\partial \theta_i^T}{\partial z} M_{iq} \qquad (3\text{-}17)$$

For a linear equilibrator (par. 1-3), the force F_{ik} is a constant times displacement of the spring, or from Eq. 1-1,

$$F = K \Delta \ell$$

The spring constant for a linear mechanical spring is expressed as (Ref. 5)

$$k = \frac{Gd^4}{8D^3 n} \qquad (3\text{-}18)$$

where

G = rigidity modulus

d = wire diameter

D = coil diameter

n = number of effective coils

In a linear mechanical spring equilibrator, a compression spring is generally used, rather than a tension spring, because no extra ending is necessary for installation and if failure of the spring occurs the spring will still sustain a reduced load. Figure 3-2 shows a pull-type equilibrator, which has a compression spring. Figure 3-2(a) shows an equilibrator spring

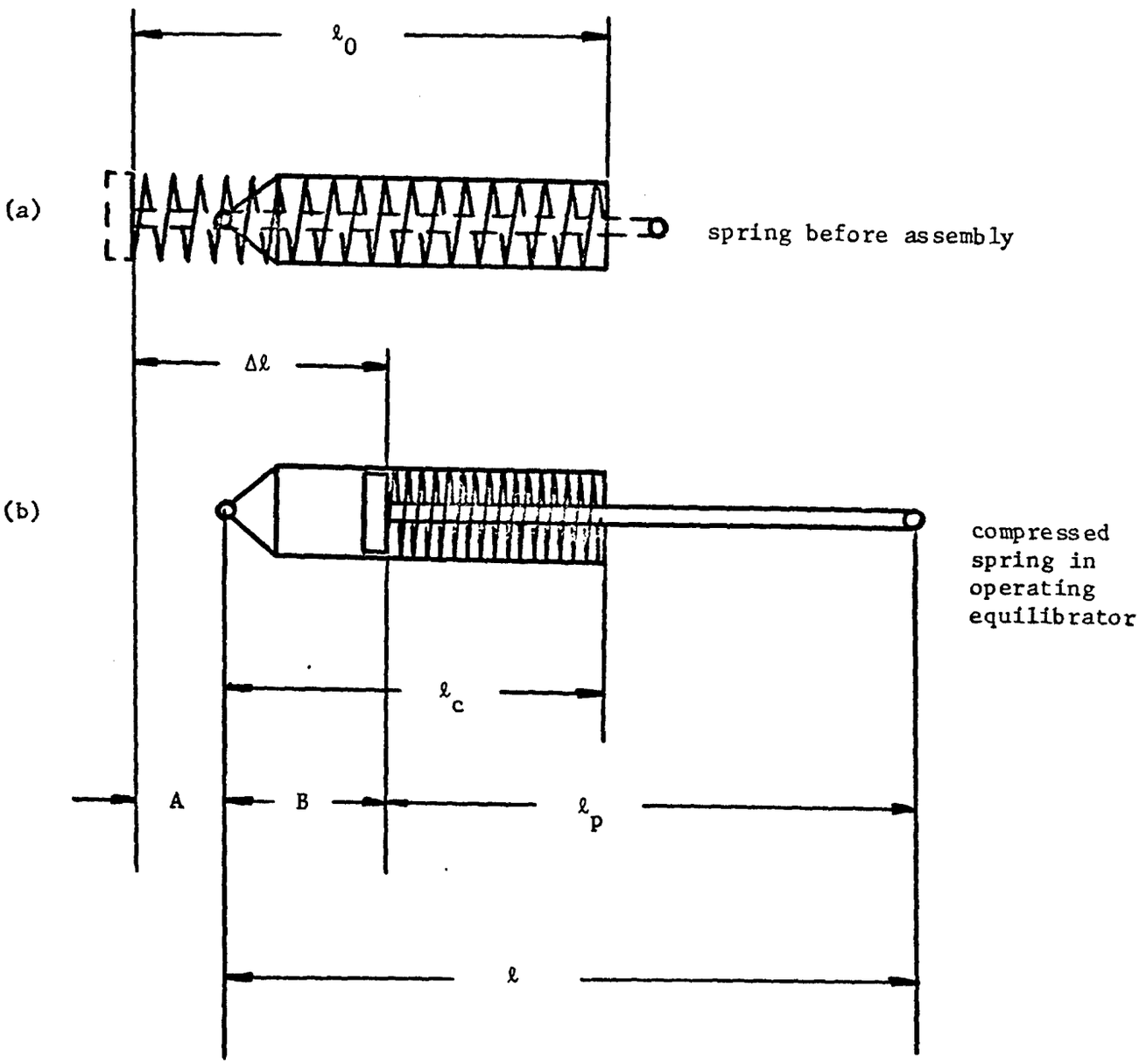

ℓ_0 = spring free length
ℓ_c = cylinder length
ℓ_p = piston length
ℓ = equilibrator length

Figure 3-2 Spring Deflection Calculation

before assembly. The spring free length is usually longer than the cylinder length, for presetting. Figure 3-2(b) shows the compressed spring when the equilibrator length is ℓ. Spring deflection is the sum of lengths A and B, which are $\ell_0 - \ell_c$ and $\ell - \ell_p$ respectively; i.e.,

$$\begin{aligned} \Delta\ell &= (\ell_0 - \ell_c) + (\ell - \ell_p) \\ &= \ell_0 - \ell_c - \ell_p + \ell \end{aligned} \tag{3-19}$$

where

ℓ_0 = spring free length

ℓ_c = cylinder length

ℓ_p = piston length

ℓ = equilibrator length

Equations 1-1, 3-18, and 3-19 determine the magnitude of the equilibrator force. The direction of the equilibrator force is

$$\vec{n} = \frac{\vec{\ell}_{ijk}}{|\vec{\ell}_{ijk}|} \tag{3-20}$$

where $\vec{n}$ = direction vector

Exploiting Eqs. 1-1, 3-18, 3-19 and 3-20, the first term on the right side of Eq. 3-17 becomes

$$\sum_{k=1}^{r} \frac{\partial(-\ell_{ijk})^T}{\partial z} \left(\frac{\vec{\ell}_{ijk}}{|\vec{\ell}_{ijk}|}\right) \left(\frac{G_k d_k^4}{8D_k^3 n_k}\right) \left(\ell_{0_k} - \ell_{c_k} - \ell_{pk} + \ell_k\right) \tag{3-21}$$

where k represents the kth equilibrator.

CHAPTER 4

OPTIMAL DESIGN PROBLEM FORMULATION

4-1 Statement of the Optimal Design Problem

The optimal design problem for a force-balancing mechanism can be stated as follows:

Find $b \in R^k$ to minimize the cost function

$$\psi_0 = \psi_0(b) \tag{4-1}$$

subject to the constraints;

(i) state equation for position, from Eq. 2-3,

$$\Phi(z, b, \alpha) = 0 \tag{4-2}$$

(ii) force equation, from Eq. 3-12

$$\frac{\partial \Phi^T(z, b, \alpha)}{\partial \bar{z}} \mu = G(z, \alpha, b) \tag{4-3}$$

(iii) composite design constraints

$$\max_{\alpha} \ \psi_i(z, \mu(b, \alpha)) \leq 0, \quad i = 1, \ldots, p \tag{4-4}$$

where p is the total number of design constraints.

4-2 Discretized Problem

The optimal design problem stated in the previous paragraph is valid on the entire range of α. Such problems are called parametric optimal design problems. Techniques for handling parametric optimal design problems have been developed in Ref. 1. One simple way of handling this problem is to discretize α into finite number of grid points. The composite design constraints are required to hold at every grid point on the α-grid, so the generalized force must be calculated at every grid point. Thus the state

equation, force equation, and composite design constraints can be rewritten as

$$\Phi(a, b, \alpha^j) = 0, \quad j = 1, \ldots, t' \tag{4-5}$$

$$\frac{\partial \Phi(z, b, \alpha^j)^T}{\partial z} \mu = G(z, b, \alpha^j), \quad j = 1, \ldots, t' \tag{4-6}$$

$$\max_j \ \psi_i(z, \mu(b, \alpha^j), b) \leq 0, \quad i = 1, \ldots, p, \quad j = 1, \ldots, t' \tag{4-7}$$

where t' is the total number of grid points of α.

4-3 A Reformulation of the Problem

It is now necessary to define the cost function more precisely. In a static force-balancing mechanism, the eventual aim is to minimize the deviation between the balancing force and the force to be balanced. Since this imbalance varies as the environmental parameter α varies, the maximum unbalance is chosen to be minimized. One can now introduce an artificial design parameter b_{k+1} to satisfy the constraint

$$\max_j f(z, \mu(\alpha^j, b), b) - b_{k+1} \leq 0 \quad j = 1, \ldots, t' \tag{4-8}$$

where f is the unbalance between the balancing force and the force to be balanced. This upper bound on the maximum unbalance can be modified as

$$\psi_0(b) = b_{k+1} \tag{4-9}$$

with the additional constraint of Eq. 4-8.

Since the range of α is being discretized, the constraints must be evaluated at each α-grid point to determine violations in the constraints. The relative maximum strategy (see Par. 4-5) is used for the constraint equations of Eqs. 4-7 and 4-8.

The optimal design problem may now be restated as:

Find $b \in R^{k+1}$ to minimize the cost function

$$\psi_0 = b_{k+1} \tag{4-10}$$

subject to the constraints;

(i) state equation for position, from Eq. 4-5,

$$\Phi(z, b, \alpha^j) = 0, \quad j = 1, \ldots, t' \tag{4-11}$$

(ii) force equation, from Eq. 4-6,

$$\frac{\partial \Phi(z, b, \alpha^j)^T}{\partial z} \mu = G(z, b, \alpha^j), \quad j = 1, \ldots, t' \tag{4-12}$$

(iii) composite design constraint

$$\psi_i(z, \mu(b, \alpha^j), b) \leq 0, \quad i = 1, \ldots, p \quad j = 1, \ldots, t' \tag{4-13}$$

where t' is the total number of grid points of α.

4-4 Design Sensitivity Analysis

Derivatives of the cost function and constraint equations with respect to design variables must be calculated before any optimization algorithm is applied. The idea of design sensitivity analysis is to construct an approximation of the design problem that can be analyzed to determine the effect of a change δb in b^0. The approximate problem is obtained by making linear approximations to nonlinear functions. A linear approximation to the change in ψ_0 is trivial and linear approximations to changes in ψ_i, due to the small changes in all variables, are

$$\delta\psi_i = \frac{\partial \psi_i}{\partial z} \delta z + \frac{\partial \psi_i}{\partial \mu} \delta\mu + \frac{\partial \psi_i}{\partial b} \delta b \tag{4-14}$$

To construct a design sensitivity vector is to find the vector ℓ^i as

$$\delta\psi_i = \ell^{i^T} \delta b \tag{4-15}$$

Hence, it is necessary to express δz and $\delta\mu$ in terms of δb. To get the relation between δz and δb, take the first variation of Eq. 4-11, with α fixed, to obtain

$$\frac{\partial \Phi}{\partial z} \delta z + \frac{\partial \Phi}{\partial b} \delta b = 0 \tag{4-16}$$

Since $\frac{\partial \Phi}{\partial z}$ is non-singular (see Par. 2-2),

$$\delta z = \left(-\frac{\partial \Phi}{\partial z}\right)^{-1} \frac{\partial \Phi}{\partial b} \delta b \tag{4-17}$$

The first term of Eq. 4-14 thus becomes

$$\frac{\partial \psi_i}{\partial z} \delta z = -\frac{\partial \psi_i}{\partial z} \left(\frac{\partial \Phi}{\partial z}\right)^{-1} \frac{\partial \Phi}{\partial b} \delta b \tag{4-18}$$

Defining an adjoint variable λ_i^1 such that

$$\lambda_i^{1^T} = -\frac{\partial \psi_i}{\partial z} \left(\frac{\partial \Phi}{\partial z}\right)^{-1} \tag{4-19}$$

reduces the cost of computation by avoiding calculation of the inverse matrix $\left(\frac{\partial \Phi}{\partial z}\right)^{-1}$; i.e., λ_i^1 is the solution of adjoint equation

$$\left(\frac{\partial \Phi}{\partial z}\right)^T \lambda_i^1 = -\left(\frac{\partial \psi_i}{\partial z}\right)^T \tag{4-20}$$

Now, Eq. 4-18 becomes

$$\frac{\partial \psi_i}{\partial z} \delta z = \lambda_i^1 \frac{\partial \Phi}{\partial b} \delta b \tag{4-21}$$

One can also express $\delta\mu$ in terms of δb by taking the first variation of Eq. 4-12, keeping b invariant,

$$\frac{\partial\left[\left(\frac{\partial\Phi}{\partial z}\right)^T\mu\right]}{\partial z}\,\delta z + \left(\frac{\partial\Phi}{\partial z}\right)^T \delta\mu = \frac{\partial G}{\partial z}\,\delta z + \frac{\delta G}{\delta b}\,\delta b \tag{4-22}$$

This equation yields

$$\delta\mu = \left[\left(\frac{\partial\Phi}{\partial z}\right)^T\right]^{-1}\left[\left\{\frac{\partial G}{\partial z} - \frac{\partial\left[\left(\frac{\partial\Phi}{\partial z}\right)^T\mu\right]}{\partial z}\right\}\delta z + \frac{\partial G}{\partial b}\,\delta b\right] \tag{4-23}$$

The second term of Eq. 4-14 thus becomes

$$\frac{\partial\psi_i}{\partial\mu}\,\delta\mu = \frac{\partial\psi_i}{\partial\mu}\left[\left(\frac{\partial\Phi}{\partial z}\right)^T\right]^{-1}\left[\left\{\frac{\partial G}{\partial z} - \frac{\partial\left[\left(\frac{\partial\Phi}{\partial z}\right)^T\mu\right]}{\partial z}\right\}\delta z + \frac{\partial G}{\partial b}\,\delta b\right] \tag{4-24}$$

Similarly to Eq. 4-19, define an adjoint variable λ_i^2 as

$$\lambda_i^{2^T} = \left(\frac{\partial\psi_i}{\partial\mu}\right)\left[\left(\frac{\partial\Phi}{\partial z}\right)^T\right]^{-1} \tag{4-25}$$

This can be rewritten as

$$\frac{\partial\Phi}{\partial z}\,\lambda_i^2 = \left(\frac{\partial\psi_i}{\partial\mu}\right)^T \tag{4-26}$$

Using Eq. 4-17 and 4-25, Eq. 4-24 becomes

$$\frac{\partial\psi_i}{\partial\mu}\,\delta\mu = \lambda_i^{2^T}\left[-\left\{\frac{\partial G}{\partial z} - \frac{\partial\left[\left(\frac{\partial\Phi}{\partial z}\right)^T\mu\right]}{\partial z}\right\}\left(\frac{\partial\Phi}{\partial z}\right)^{-1}\frac{\partial\Phi}{\partial b}\,\delta b + \frac{\partial G}{\partial b}\,\delta b\right] \tag{4-27}$$

Defining λ_i^3 such that

$$\lambda_i^{3^T} = -\left\{\frac{\partial G}{\partial z} - \frac{\partial\left[\left(\frac{\partial\Phi}{\partial z}\right)^T\mu\right]}{\partial z}\right\}\left(\frac{\partial\Phi}{\partial z}\right)^{-1} \tag{4-28}$$

one can rewrite Eq. 4-27 as

$$\frac{\partial \psi_i}{\partial \mu} \delta\mu = \lambda_i^{2^T} \left[\lambda_i^{3^T} \frac{\partial \Phi}{\partial b} + \frac{\partial G}{\partial b} \right] \delta b \tag{4-29}$$

and λ_i^3 is the solution of

$$\left(\frac{\partial \Phi}{\partial z}\right)^T \lambda_i^3 = - \left\{ \frac{\partial G}{\partial z} - \frac{\partial \left[\left(\frac{\partial \Phi}{\partial z} \right)^T \mu \right]}{\partial z} \right\}^T \tag{4-30}$$

Substituting Eqs. 4-21 and 4-29 into Eq. 4-14, one finally has

$$\delta \psi_i = \left\{ \left[\lambda_i^{1^T} + \lambda_i^{2^T} \lambda_i^{3^T} \right] \frac{\partial \Phi}{\partial b} + \lambda_i^{2^T} \frac{\partial G}{\partial b} + \frac{\partial \psi_i}{\partial b} \right\} \delta b \equiv \ell^{i^T} \delta b \tag{4-31}$$

The design sensitivity vector is thus

$$\ell^{i^T} = \left[\lambda_i^1 + \lambda_i^{2^T} \lambda_i^{3^T} \right] \left(\frac{\partial \Phi}{\partial b} \right) + \lambda^{2^T} \frac{\partial G}{\partial b} + \frac{\partial \psi_i}{\partial b} \tag{4-32}$$

where the adjoint variables λ_i^1, λ_i^2, and λ_i^3 are the solutions of Eqs. 4-20, 4-26, and 4-30, respectively.

4-5 Optimization Algorithm

With the design sensitivity vector calculated in the previous paragraph, one can implement an optimization algorithm of his choice. The gradient projection method with constant error correction (Ref. 1) is chosen here.

Among the constraint equations of Eq. 4-13, some are dependent on the environmental parameter α. Such constraints are called parametric constraints. Constraints that are independent of the environmental parameter are called nonparametric constraints. This distinction is necessary to save calculations, because one does not need to calculate nonparametric constraints at every grid point. Enforcing constraints only at relative maxima in α, called the relative maximum strategy, decreases the number of

calculations even further. This strategy chooses the grid point at which the relative maximum violation of a constraint occurs and solves the state equations only at that point and in a neighborhood of the point. This is called a non-sweep iteration. The actual computational optimization algorithm is presented in Chapter 3 of Ref. 2 as follows:

Step 1 : Estimate a design b^0 and impose a grid on the range of the input parameter α.

Step 2 : Solve the state equations of Eq. 4-11 and 4-12 for $z(\alpha^j)$ and $\mu(\alpha^j)$, respectively.

Step 3 : Check all non-parametric and parametric design constraints. Form a reduced vector $\tilde{\psi}$ consisting of all ε-active non-parametric constraints and relative maxima of ε-active parametric constraints.

Step 4 : Compute the adjoint variables λ^1_{ij}, λ^2_{ij}, and λ^3_{ij} from Eqs. 4-20, 4-26, and 4-30, associated only with the constraint functions in $\tilde{\psi}$. Construct ℓ^{i^T} of Eq. 4-32 for each of these constraint functions. Form the matrix $\Lambda = [\ell^{ij}]$, whose columns are the vectors ℓ^{i^T} corresponding to constraint functions in $\tilde{\psi}$. Thus, $\delta\tilde{\psi} = \Lambda^T \delta b$.

Step 5 : Compute the vector $M_{\psi\psi}$ and the matrix $M_{\psi\psi}$ from the following relations:

$$M_{\psi\psi_0} = \Lambda^T W^{-1} \ell^0 \tag{4-33}$$

where ℓ^0 is obtained from the variation of cost function as

$$\delta\psi_0 = \frac{\partial\psi_0}{\partial b}\,\delta b \equiv \ell^{0^T}\delta b \tag{4-34}$$

$$M_{\psi\psi} = \Lambda^T W^{-1} \Lambda \tag{4-35}$$

Step 6 : Compute a parameter γ, related to step size, as

$$\gamma = \frac{\ell^{0^T} W^{-1} \ell^0}{2\beta \psi_0(b^0)} \tag{4-36}$$

where β is the desired fractional reduction in the cost function. The usual range of β is 0.03 to 0.15.

Step 7 : Compute $\tilde{\mu}^1$ and $\tilde{\mu}^2$ from

$$M_{\psi\psi} \tilde{\mu}^1 = - M_{\psi\psi_0} \tag{4-37}$$

$$M_{\psi\psi} \tilde{\mu}^2 = \tilde{\psi} \tag{4-38}$$

Step 8 : Compute δb^1 and δb^2 from

$$\delta b^1 = W^{-1} [\ell + \Lambda \tilde{\mu}^1] \tag{4-39}$$

$$\delta b^2 = - W^{-1} \Lambda \tilde{\mu}^2 \tag{4-40}$$

Step 9 : Compute an update in design δb from

$$\delta b = - \frac{1}{2\gamma} \delta b^1 + \delta b^2 \tag{4-41}$$

Step 10 : Update the estimate of the optimum design to

$$b^1 = b^0 + \delta b \tag{4-42}$$

Step 11 : If all constraints are satisfied, to within the prescribed tolerance, and

$$||\delta b^1|| = \left[\sum_{i=1}^{m} W_i (\delta b^1)^2 \right]^{1/2} \leq \delta \tag{4-43}$$

terminate the process. Otherwise, return to step 2, with b^1 as the new estimate for b.

CHAPTER 5

APPLICATIONS

5-1 A Linear Mechanical Spring Weapon Equilibrator

As an example calculation, a linear mechanical spring equilibrator for a weapon is designed. Two concentric springs are installed. Their direction of winding is opposite, to prevent the inner spring from interlacing with the outer spring. Both cylinder wall and piston rod work as guides to prevent buckling.

Figure 5-1(a) shows geometry of the equilibrator and the definitions of global and local coordinates. Figure 5-1(b) shows dimensions in the initial position. Body I (top carriage) is the weapon support and body II (tipping parts) is connected to body I at the trunnion (a revolute joint). This system has only one moving body, hence the total number of degrees-of-freedom is 3. One revolute joint gives rise to two state equations in Eq. 2-5. Therefore this system has one free degree-of-freedom and has one driving constraint, which is written in the form

$$\theta - \alpha_j = 0 \qquad j = 1, \ldots, t' \tag{5-1}$$

where

θ = elevation angle

α_j = given values at grid point j

t' = total number of grids

Equations 2-5 and 5-1 form the state equations (Eq. 4-11).

The inner and outer springs are installed in the same equilibrator, hence there is only one equilibrator length vector $\vec{\ell}$. The force equation of Eq. 3-21 becomes

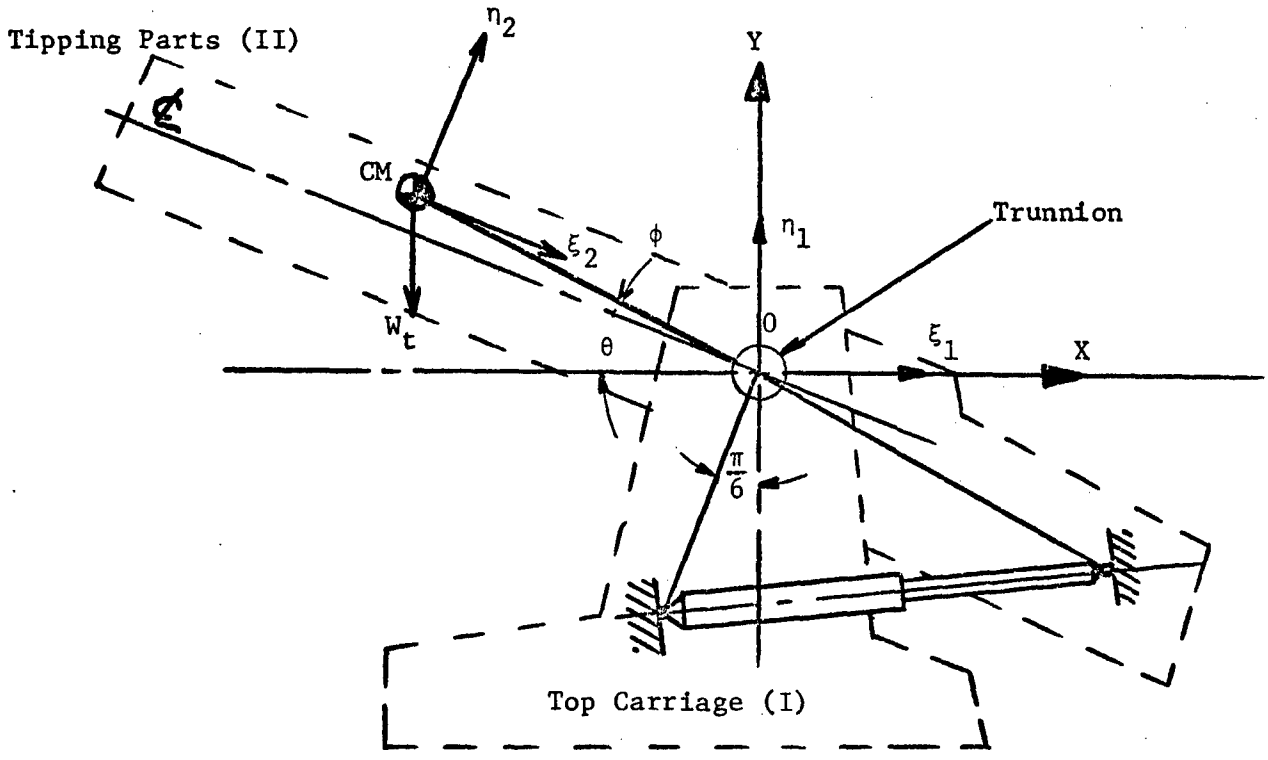

(a) Geometry of Equilibrator

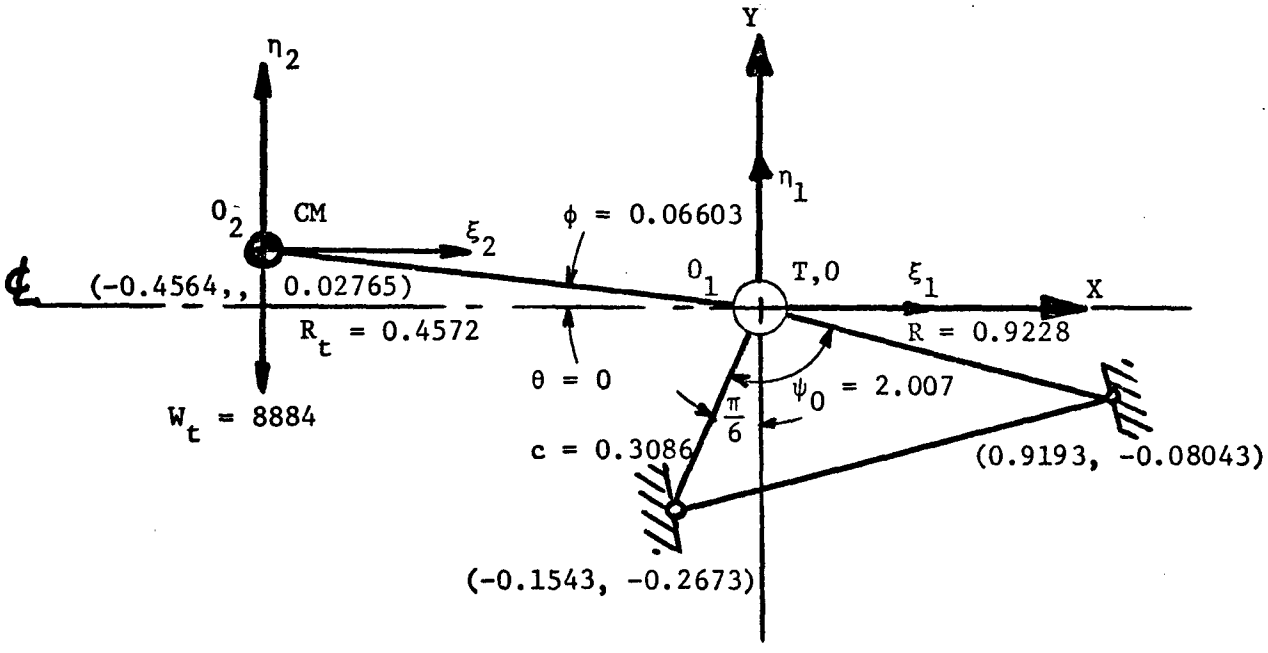

(b) Initial Condition of Equilibrator
Force in N, Length in m and Angle in Radian

Figure 5-1 Geometry of Weapon Equilibrator

$$G = \frac{\partial(-\ell)^T}{\partial z}\left(\frac{\vec{\ell}}{|\vec{\ell}|}\right)\left\{\frac{Gd_1^4}{8D_1^3 n_1}\left(\ell_{0_1} - \ell_c - \ell_p + |\vec{\ell}|\right)\right.$$

$$\left. + \frac{Gd_2^4}{8D_2^3 n_2}\left(\ell_{0_2} - \ell_c - \ell_p + |\vec{\ell}|\right)\right\} \qquad (5\text{-}2)$$

The design variables are chosen as spring wire diameters, numbers of effective coils, and pitches; i.e.

$$\left.\begin{aligned} b_1 &= d_1 \\ b_2 &= n_1 \\ b_3 &= p_1 \\ b_4 &= d_2 \\ b_5 &= n_2 \\ b_6 &= p_2 \end{aligned}\right\} \qquad (5\text{-}3)$$

where d_1, d_2 = wire diameters of spring 1, 2

n_1, n_2 = number of effective coils of springs 1, 2

p_1, p_2 = pitches of spring 1, 2

Noting that the spring free length is the number of active coils times pitch and using Eq. 5-3, Eq. 5-2 becomes

$$G = \frac{\partial(-\ell)^T}{\partial \vec{z}}\left(\frac{\vec{\ell}}{|\vec{\ell}|}\right)\left\{4.18 \times 10^{12}\,\frac{b_1^4}{b_2}\left(b_3\, b_2 + \ell_j - 1.41\right)\right.$$

$$\left. + 1.41 \times 10^{13}\,\frac{b_4^4}{b_5}\left(b_6\, b_5 + \ell_j - 1.41\right)\right\} \qquad (5\text{-}4)$$

where $G = 7.93 \times 10^{10}$ Pa

$D_1 = 0.13335$ m

$D_2 = 0.889$ m

$\ell_c = 0.7$ m

$\ell_p = 0.71$ m

The inner spring is required to support 40% of the outer spring load. This force distribution gives the constraint

$$0.1185 \frac{b_1^4}{b_2} (b_3 b_2 + \ell_j - 1.41) - \frac{b_4^4}{b_5} (b_6 b_5 + \ell_j - 1.41) \leq 0 \quad (5\text{-}5)$$

where numberical values of G, D_1, D_2, ℓ_c, and ℓ_p are substituted.

The shear stress of a spring under load P is (Ref. 5)

$$\tau = \frac{8PD}{\pi d^3} \quad (5\text{-}6)$$

Allowable stress is taken as $\tau_a = 9.1 \times 10^8$ Pa (Ref. 5) and

$$\left.\begin{aligned} P_1 &= F/1.4 \\ P_2 &= 0.4F/1.4 \end{aligned}\right\} \quad (5\text{-}7)$$

are the loads for springs 1 and 2, where

F = equilibrator force

Substituting P_1 and P_2 and using $\tau_a = 9.1 \times 10^8$ Pa, the two stress constraints are

$$\left.\begin{aligned} 1559.8 \frac{b_1}{b_2} (b_3 b_2 + \ell_j - 1.41) - 1 &\leq 0 \\ 3508.8 \frac{b_4}{b_5} (b_6 b_5 + \ell_j - 1.41) - 1 &\leq 0 \end{aligned}\right\} \quad (5\text{-}8)$$

This optimization problem may now be stated as follows:

Find $b \in R^7$ to minimize

$$\psi_0 = b_7$$

subject to state equations of Eq. 4-11, force equation of Eq. 5-4, constraint equations of Eqs. 5-5 and 5-8, and

$$|\mu_6| - b_7 \leq 0 \tag{5-9}$$

where μ_6 is the constraint force in the z_6 direction; i.e., the direction of rotation of the tipping parts. This is interpreted as the unbalance between the weight moment of the tipping parts and the equilibrator torque.

The starting values of design parameters were taken as shown in Table 5-1. This resulted in $||\delta b^1|| = 160.7$, $||\delta b^2|| = 13.14$, and a cost function value of 51.24. The constraint of Eq. 5-9 was violated and other constraints were active at some grid points. After 11 iterations, the constraint of Eq. 5-9 became active. After 20 iterations, $||\delta b^1|| = 2.55 \times 10^{-11}$, $||\delta b^2|| = 1.46 \times 10^{-3}$, and the cost function value was 94.29. All the constraints are satisfied, but are active at some grid points. The total computing time for 20 iterations on an IBM 370/168 was 35.3 sec. The cost function history is shown in Fig. 5-2.

Table 5-1 Result for the Weapon Equilibrator Design

	Starting Values	Optimum Design	Conventional Design*
d_1 m	0.0165	0.01663	0.0171
n_1	13.9	13.84	13.7
P_1 m	0.0631	0.06247	
d_2 m	0.0108	0.0109	0.0101
n_2	19.7	19.83	18.1
P_2 m	0.0426	0.04232	
max moment unbalance Nm	51.2**	94.29	245

*See Ref. 6.

**Infeasible design

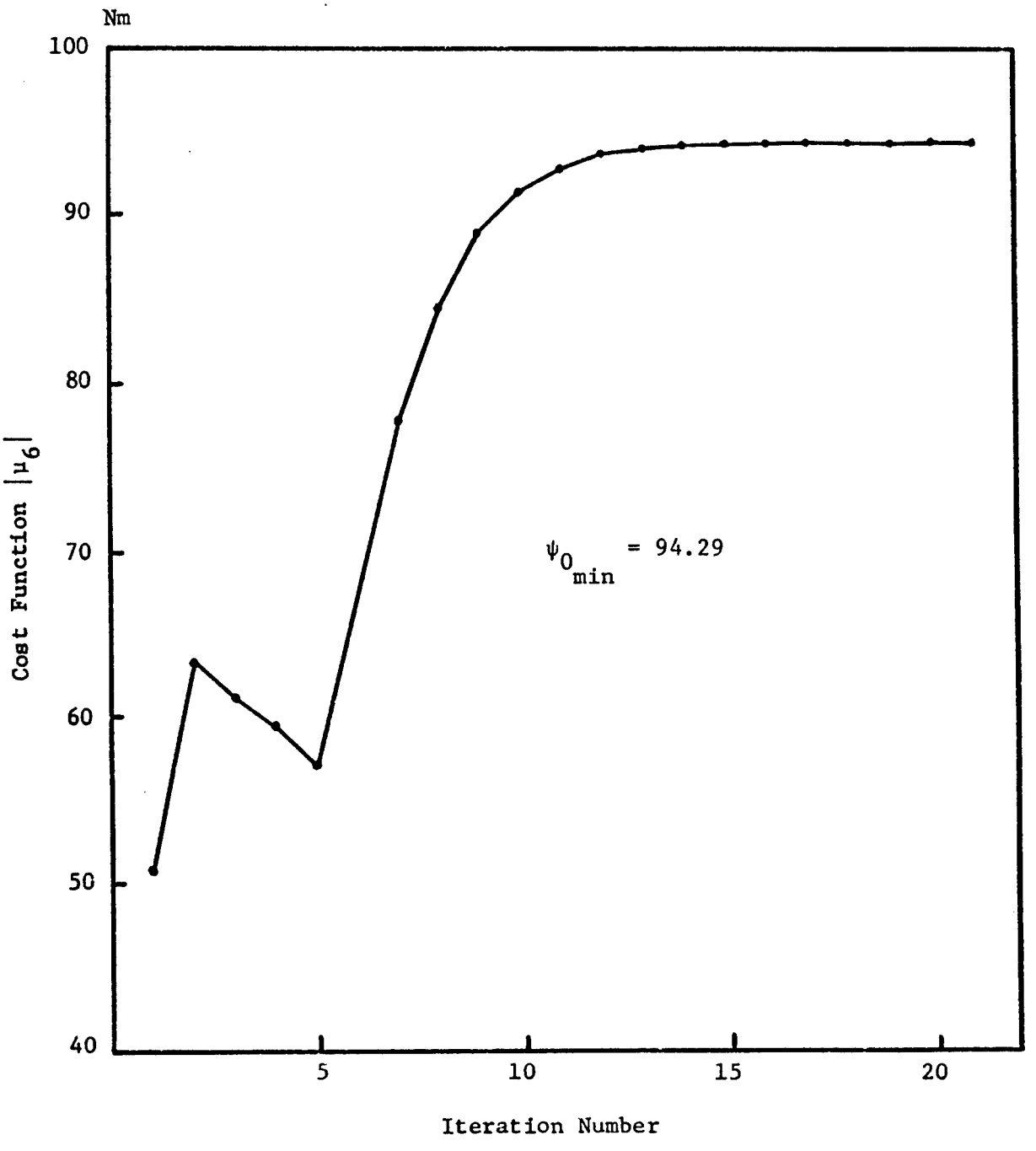

Figure 5-2 Cost Function History of the Weapon Equilibrator

REFERENCES

1. Haug, E.J., and Arora, J.S., Applied Optimal Design Mechanical and Structural Systems, John Wiley & Sons, 1979.

2. Sohoni, V, and Haug, E.J., A State Space Technique for Kinematic Synthesis of Planar Mechanisms and Machines, Technical Report No. 81-5, Center for Computer Aided Design, College of Engineering, The University of Iowa, Iowa City, Iowa, September, 1981.

3. Taylor, A.E., Advanced Calculus, Guinn, Boston, 1955.

4. Greenwood, D.T., Principles of Dynamics, Prentice-Hall, Inc., 1965.

5. Wahl, A.M., Mechanical Springs, McGraw-Hill Book Company, Inc., 1963.

6. DARP 706-XXX, Engineering Design Handbook, Design of Towed Artillery Systems, HQ US Army Material Command, Alexandria, Va., to appear 1982.

DISTRIBUTION LIST

Please notify USATACOM, DRSTA-ZSA, Warren, Michigan 48090, of corrections and/or changes in address.

Commander (25)
US Army Tk-Autmv Command
R&D Center
Warren, MI 48090

Superintendent (02)
US Military Academy
ATTN: Dept of Engineering
Course Director for
Automotive Engineering

Commander (01)
US Army Logistic Center
Fort Lee, VA 23801

US Army Research Office (02)
P.O. Box 12211
ATTN: Dr. F. Schmiedeshoff
Dr. R. Singleton
Research Triangle Park, NC 27709

HQ, DA (01)
ATTN: DAMA-AR
Dr. Herschner
Washington, D.C. 20310

HQ, DA (01)
Office of Dep Chief of Staff
for Rsch, Dev & Acquisition
ATTN: DAMA-AR
Dr. Charles Church
Washington, D.C. 20310

HQ, DARCOM
5001 Eisenhower Ave.
ATTN: DRCDE
Dr. R.L. Haley
Alexandria, VA 22333

Director (01)
Defense Advanced Research
Projects Agency
1400 Wilson Boulevard
Arlington, VA 22209

Commander (01)
US Army Combined Arms Combat
Developments Activity
ATTN: ATCA-CCC-S
Fort Leavenworth, KA 66027

Commander (01)
US Army Mobility Equipment
Research and Development Command
ATTN: DRDME-RT
Fort Belvoir, VA 22060

Director (02)
US Army Corps of Engineers
Waterways Experiment Station
P.O. Box 631
Vicksburg, MS 39180

Commander (01)
US Army Materials and Mechanics
Research Center
ATTN: Mr. Adachi
Watertown, MA 02172

Director (03)
US Army Corps of Engineers
Waterways Experiment Station
P.O. Box 631
ATTN: Mr. Nuttall
Vicksburg, MS 39180

Director (04)
US Army Cold Regions Research
& Engineering Lab
P.O. Box 282
ATTN: Dr. Freitag, Dr. W. Harrison
Dr. Liston, Library
Hanover, NH 03755

Grumman Aerospace Corp (02)
South Oyster Bay Road
ATTN: Dr. L. Karafiath
Mr. F. Markow
M/S A08/35
Bethpage, NY 11714

Dr. Bruce Liljedahl (01)
Agricultural Engineering Dept
Purdue University
Lafayette, IN 46207

Mr. H.C. Hodges (01)
Nevada Automotive Test Center
Box 234
Carson City, NV 89701

Mr. R.S. Wismer (01)
Deere & Company
Engineering Research
3300 River Drive
Moline, IL 61265

Oregon State University (01)
Library
Corvallis, OR 97331

Southwest Research Inst (01)
8500 Culebra Road
San Antonia, TX 78228

FMC Corporation (01)
Technical Library
P.O. Box 1201
San Jose, CA 95108

Mr. J. Appelblatt (01)
Director of Engineering
Cadillac Gauge Company
P.O. Box 1027
Warren, MI 48090

Chrysler Corporation (02)
Mobility Research Laboratory,
Defense Engineering
Department 6100
P.O. Box 751
Detroit, MI 48231

CALSPAN Corporation (01)
Box 235
Library
4455 Benesse Street
Buffalo, NY 14221

SEM, (01)
Forsvaretsforskningsanstalt
Avd 2
Stockholm 80, Sweden

Mr. Hedwig (02)
RU III/6
Ministry of Defense
5300 Bonn, Germany

Foreign Science & Tech (01)
Center
220 7th Street North East
ATTN: AMXST-GEI
Mr. Tim Nix
Charlottesville, VA 22901

General Research Corp (01)
7655 Old Springhouse Road
Westgate Research Park
ATTN: Mr. A. Viilu
McLean, VA 22101

Commander (01)
US Army Developmant and
Readiness Command
5001 Eisenhower Avenue
ATTN: Dr. R.S. Wiseman
Alexandria, VA 22333

President (02)
Army Armor and Engineer Board
Fort Knox, KY 40121

Commander (01)
US Army Arctic Test Center
APO 409
Seattle, WA 98733

Commander (02)
US Army Test & Evaluation
Command
ATTN: AMSTE-BB and AMSTE-TA
Aberdeen Proving Ground, MD
21005

Commander (01)
US Army Armament Research
and Development Command
ATTN: Mr. Rubin
Dover, NJ 07801

Commander (01)
US Army Yuma Proving Ground
ATTN: STEYP-RPT
Yuma, AZ 85364

Commander (01)
US Army Natic Laboratories
ATTN: Technical Library
Natick, MA 01760

Director (01)
US Army Human Engineering Lab
ATTN: Mr. Eckels
Aberdeen Proving Ground, MD
21005

Director (02)
US Army Ballistic Research Lab
Aberdeen Proving Ground, MD
21005

Director (02)
US Army Materiel Systems
Analysis Agency
ATTN: AMXSY-CM
Aberdeen Proving Ground, MD
21005

Director (02)
Defense Documentation Center
Cameron Station
Alexandria, VA 22314

US Marine Corps (01)
Mobility & Logistics Division
Development and Ed Command
ATTN: Mr. Hickson
Quantico, VA 22134

Keweenaw Field Station (01)
Keweenaw Research Center
Rural Route 1
P.O. Box 94-D
ATTN: Dr. Sung M. Lee
Calumet, MI 49913

Naval Ship Research & (02)
Dev Center
Aviation & Surface Effects Dept
Code 161
Washington, D.C. 20034

Director (01)
National Tillage Machinery Lab
Box 792
Auburn, AL 36830

Director (02)
USDA Forest Service Equipment
Development Center
444 East Bonita Avenue
San Dimes, CA 91773

Engineering Societies (01)
Library
345 East 47th Street
New York, NY 10017

Dr. I.R. Erlich (01)
Dean for Research
Stevens Institute of Technology
Castle Point Station
Hoboken, NJ 07030